IBRACON

**IBRACON Structures and Materials Journal**
Revista IBRACON de Estruturas e Materiais
ISSN 1983-4195 *ismj.org*

SciELO

ORIGINAL ARTICLE

# Post punching shear pattern and progressive collapse of flat slab building

*Comportamento pós punção e colapso progressivo em uma estrutura em laje lisa*

Bernardo Cruz Pereira Galdino[a]
Guilherme Sales Melo[a]

[a]Universidade de Brasília – UnB, Department of Civil and Environmental Engineering, Brasília, DF, Brasil

Received 23 June 2022
Accepted 23 March 2023

**Abstract:** The possibility of the occurrence of a second punching shear failure and of a Progressive Collapse after a punching shear failure had occurred in one flat slab column connection is investigated in two building structures, using Eberick and SAP2000 softwares and the Yield Line Method, and codes ACI318:2019, EUROCODE2:2004 and NBR6118:2014. It is shown that slab column connections should be designed and detailed to prevent Progressive Collapse and that Integrity Reinforcement should always be present, and that the remaining capacity of floors after punching failures depends on the *i)* post-punching resistance of the connection being punched; *ii)* post-punching resistance of the neighbors' connections; *iii)* flexural resistance of the slabs, and that the flexural resistance of the slab's floors can be evaluated by the Yield Line Method.

**Keywords:** progressive collapse, flat slab, punching shear, yield line theory.

**Resumo:** A possibilidade da ocorrência de uma segunda ruptura por punção e colapso progressivo depois de uma ruptura por punção em uma ligação laje-pilar foi investigado em duas estruturas, usando os softwares Eberick e SAP2000, Método das Linhas de Ruptura e as normas ACI318:2019, EUROCODE2:2004 e NBR6118:2014. Verifica-se que a ligação laje-pilar deve ser projetada para prevenir o colapso progressivo, as armaduras contra o colapso progressivo devem estar sempre presentes, a capacidade remanescente da laje lisa depois de uma ruptura por punção depende da resistência pós punção da ligação puncionada, resistência pós punção das ligações vizinhas sobrecarregadas, resistência de flexão da laje conforme o Método das Linhas de Ruptura.

**Palavras-chave:** colapso progressivo, laje lisa, punção cisalhante, linhas de ruptura.

**How to cite:** B. C. P. Galdino and G. S. Melo, "Post punching shear pattern and progressive collapse of flat slab building," *Rev. IBRACON Estrut. Mater.*, vol. 16, no. 3, e16312, 2023, https://doi.org/10.1590/S1983-41952023000300012

## 1 INTRODUCTION

This study aims to verify using a software the post-punching shear behavior of reinforced concrete flat slab structures considering the partial or total failure of the slab-column connection, using SAP 2000 [1] and Eberick 2022 [2] software's.

When a slab-column connection fails, there may be an overload on neighboring supports and new failures may occur in a chain reaction [3]. Thus, the effect known as progressive collapse arises.

The causes of this phenomenon include improper renovation of structure, fire, vehicle collision, substandard material, design and/or execution errors. The accident that occurred with the Liberdade Building, in Rio de Janeiro, highlights the tragic damage caused after the loss of a support [4].

Progressive collapse of a building can be trigged by a punching shear failure even eight months after a slab-column connection punching shear resistance was exceeded by almost four times [5].

**Corresponding author:** Bernardo Cruz Pereira Galdino. E-mail: eng.bernardogaldino @gmail.com
**Financial support:** None.
**Conflict of interest:** Nothing to declare.
**Data Availability:** The data that support the findings of this study are available from the corresponding author, [B.C.P. Galdino], upon reasonable request.

Flat slabs are structural elements that are rested by columns and are very susceptible to progressive collapse, as there is less capacity for redistribution of loads and a brittle failure by punching with few pathology warnings. The advantages of using this structural system are lower ceiling heights, concrete forms simplifications and lower costs during construction.

In order to avoid progressive collapse and improve post-punching shear behavior, well anchored reinforcement can be used at the bottom of slab-column connections and is necessary to create alternative load paths, ductility, and continuity in the structure [6], [7], and this integrity bottom reinforcement is required and adopted in most codes [8]–[10].

The utilization of the Yield Line Theory to evaluate the post punching capacity of a flat floor submitted to a punching shear failure and its relation to the possibility of the occurrence of a progressive collapse has been adopted for some time [6], [11], and this use has been continued [12].

And as progressive collapse is not a well comprehensively explored phenomenon, due to its many implications [13], investigations continue to being done on the subject [14], [15], as post-punching shear behavior is one of the main factors that will interfere on the behavior of the floor slab and on the possibility of a progressive collapse and its possible tragic consequences.

## 2 METHODOLOGIES

Two flat slab buildings structures are analyzed, first the support reactions are obtained, then one column is removed, simulating a punching shear failure at this connection, and the redistribution of the support reactions at the remaining columns are followed, checking for the possibility of a progressive collapse at all slab columns connections.

After the slab punching shear failure, the loads found were compared with the loads obtained according to the intact structure, thus verifying the increase or decrease of the reactions at the connections.

It was then analyzed if there was a possibility of new failures at the most loaded connections by means of a new verification of the punching shear, considering the acting and the shear strength stresses.

The possibility of punching shear failures was checked using the codes ACI 318 [16], EUROCODE [9] and NBR 6118 [10], according to its requirements regarding critical surfaces, punching shear reinforcement, and checking the possibility of splitting or crushing of the concrete.

According to NBR 6118 [10], with the presence of shear reinforcement at the column region there are three calculated design stresses ($\tau_{Sd1}$, $\tau_{Sd2}$, $\tau_{Sd3}$) determined with Equation 1, where $F_{Sd}$ = reaction at the connection; $u$ = critical perimeter; $d$ = effective height; $M_{Sdx}$ and $M_{Sdy}$= bending moments; $K_1$ and $K_2$ depends on the columns sides ratio; and $W_{p1}$ and $W_{p2}$ = plastic resistant modulus, while the resistant stresses are determined by Equations 2 to 4, where $f_{ck}$ and $f_{cd}$ = respectively the characteristic and design concrete strength; $\rho$ = reinforcement ratio; $A_{sw}$ and $s_r$ = respectively the shear reinforcement area and spacing and $f_{ywd}$ = design yielding limit.

$$\tau_{Sd} = \frac{F_{Sd}}{u \cdot d} + \frac{K_1 \cdot M_{Sdx}}{W_{p1} \cdot d} + \frac{K_2 \cdot M_{Sdy}}{W_{p2} \cdot d} \tag{1}$$

$$\tau_{Rd1} = 0.27 \cdot (1 - \frac{f_{ck}}{250}) \cdot f_{cd} \tag{2}$$

$$\tau_{Rd2} = 0.10 \cdot (1 + \sqrt{\frac{20}{d}}) \cdot (100 \cdot \rho \cdot f_{ck})^{\frac{1}{3}} + 1.5 \cdot \frac{d}{s_r} \cdot \frac{A_{sw} \cdot f_{ywd}}{u \cdot d} \tag{3}$$

$$\tau_{Rd3} = 0.13 \cdot (1 + \sqrt{\frac{20}{d}}) \cdot (100 \cdot \rho \cdot f_{ck})^{1/3} \tag{4}$$

For EUROCODE [9] the three calculated design stresses ($\sigma_{Sd1}$, $\sigma_{Sd2}$ e $\sigma_{Sd3}$) are determined by Equation 5, similar to Equation 1, according to Equations 6 to 8, similar to Equations 2 to 4, but with a limit for a size effect on the slab thickness and a higher load factor.

$$\sigma_{Sd} = \frac{F_{Sd}}{u \cdot d} + \frac{K_1 \cdot M_{Sdx}}{W_{p1} \cdot d} + \frac{K_2 \cdot M_{Sdy}}{W_{p2} \cdot d} \tag{5}$$

$$\sigma_{Rd1} = 0.30 \cdot (1 - \frac{f_{ck}}{250}) \cdot f_{cd} \tag{6}$$

$$\sigma_{Rd2} = 0.09 \cdot (1 + \sqrt{\frac{20}{d}}) \cdot (100 \cdot \rho \cdot f_{ck})^{\frac{1}{3}} + 1.5 \cdot \frac{d}{s_r} \cdot \frac{A_{sw} \cdot f_{ywd}}{u \cdot d} \quad (7)$$

$$\sigma_{Rd3} = 0.12 \cdot (1 + \sqrt{\frac{20}{d}}) \cdot (100 \cdot \rho \cdot f_{ck})^{1/3} \quad (8)$$

ACI 318 [16] presents Equations 9 to 13, the first for the determination of the acting and the others for the resistant shear stresses, where $V$ = load transferred by the slab; $b_o$ = critical perimeter; $M_{sc}$ = bending moment at the connection; $J_c$ = geometric property of the section; $\gamma_v$ = parcel of the moment transferred by shear and $C_{AB}$ = eccentricity of the critical perimeter; $\beta$ = ratio between the column sides and $\lambda_s$ = size effect; $f'_c$ = concrete strength; $A_v$ and $s$ = respectively the shear reinforcement area and spacing and $f_{yt}$ = design yielding limit; $\alpha_s$ depends on the column position.

$$V_u = \frac{V}{b_o \cdot d} + \frac{\gamma_v \cdot M_{SC} \cdot C_{AB}}{J_c} \quad (9)$$

$$v_n = 0.75 \cdot 0.17 \cdot \left(1 + \frac{2}{\beta}\right) \cdot \lambda_s \cdot \sqrt{f'_c} + 0.75 \cdot \frac{A_v \cdot f_{yt}}{s \cdot b_o} \quad (10)$$

$$v_n = 0.75 \cdot 0.083 \cdot \left(\frac{\alpha_s \cdot d}{b_o} + 2\right) \cdot \lambda_s \cdot \sqrt{f'_c} + 0.75 \cdot \frac{A_v \cdot f_{yt}}{s \cdot b_o} \quad (11)$$

$$v_n = 0.75 \cdot 0.25 \cdot \lambda_s \cdot \sqrt{f'_c} + 0.75 \cdot \frac{A_v \cdot f_{yt}}{s \cdot b_o} \quad (12)$$

$$v_{cout} = 0.75 \cdot 0.17 \cdot \lambda_s \cdot \sqrt{f'_c} \quad (13)$$

The reinforcement against progressive collapse (integrity reinforcement) were determined according to Equations 14 to 17, according respectively to the NBR 6118:2014 [10], GSA:2013 [17], CEB:2010 [8] e ACI 352:2011 [18], where $\alpha_{ult}$ = angle between the reinforcement and the plan of the slab; and $L_1$ e $L_2$ = spans at the two directions.

$$A_s \geq \frac{1.5 \cdot F_{Sd}}{f_{yd}} \quad (14)$$

$$A_s \geq \frac{(0.17 \cdot b \cdot d \cdot f_{cd})}{f_{yd}} \quad (15)$$

$$A_s \geq \frac{F_{Sd}}{f_{yd} \cdot (ft/fy)_k \cdot sin\alpha_{ult}} \quad (16)$$

$$A_s \geq \frac{0.5 \cdot W_u \cdot L_1 \cdot L_2}{f_{yd}} \quad (17)$$

The Yield Line Theory was also used to analyze the possibility of progressive collapse in the structure after the failure of a slab-column connection. The remaining flexural capacity of the slab was verified in the region where a support was removed using the Virtual-Work Method, procedure that has been used before [6], [11], and [12].

## 3 RESULTS AND DISCUSSIONS

### 3.1 First example

The analysis of the structure was carried out according to a structural design available in two lecture notes used in the UFMG (Federal University of Minas Gerais) course, authored by Chaves [19], and Silva [20].

The post-punching shear behavior was analyzed using the computer program SAP2000 [1] using the Finite Element Method. A comparison of the Integrity Reinforcement according to NBR 6118:2014 [10], GSA:2013 [17], CEB:2010 [8] and ACI 352:2011 [18] was also presented.

As shown in Figure 1, there is an advance of the slab at the edges (overhang) to increase the stiffness of the connection and there is no presence of beams or openings at the floor for the passage of electrical or hidro-sanitary pipes.

The reinforced concrete building has three floors, a ceiling height of 289 cm and twelve columns. The slabs were designed with a thickness of 16 cm, and with columns with a square cross section of 30 cm x 30 cm.

The concrete strength is 30 MPa and the reinforcement steel grade of 500 MPa. The Elasticity Modulus of the concrete was taken as 26072 MPa. The reinforcement adopted at the analysis was the same used at the lecture notes of UFMG [19] and [20], designed by the Equivalent Frame Method. In general bars with eight millimeters of diameter each 15 or 20 centimeters were used at the two directions, and for the connections close to the corners ten millimeters bars each 10 centimeters were used at the two directions. For the internal connections 12.5 mm bars each 12 centimeter was used at the two directions. Besides this, all connections presented punching shear reinforcement.

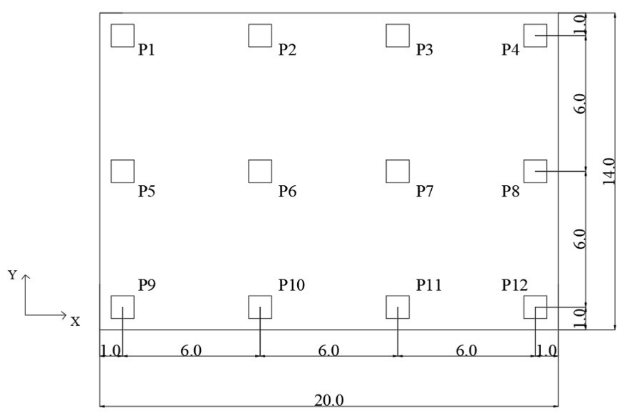


**Figure 1.** Floor plan of the structure – Dimensions in m.

According to the structural design in the lecture notes and NRB 6120 [21], a live load of 1.50 kN/m$^2$ and a total dead load of 8.08 kN/m$^2$, considering also distributed on the floor a wall located in the middle of the slab and a wall located at the periphery of the floor slab were used in the structural analysis, as shown in Table 1.

**Table 1.** Load used.

| Overview | Amount |
|---|---|
| Dead load (distributed): | Load (kN/m$^2$) |
| Self-weight of slab (h = 16.0 cm) | $25.0 \cdot 0.16 = 4.00$ |
| Cladding | 0.80 |
| Wall (middle of the slab) | 1.00 |
| Wall (periphery of the slab) | 2.28 |
| Live load: | Load (kN/m$^2$) |
| Load in residential building | 1.50 |

The slab was modeled with a “Four nodes Thin-Shell element type”, considering at the analysis only the translation normal to the slab plane. In the discretization of the slab, rectangular elements measuring 20 cm x 20 cm were used and the columns were modeled in the structural frame as frame-type connected in an element node.

Only a linear elastic structural analysis of the structure was performed, therefore, the reinforcement at columns was not determined and second-order effects were not considered.

### 3.1.1 Punching shear assessment

According to the results obtained by the codes NBR 6118:2014 [10], EUROCODE 2:2004 [9] and ACI 318:2019 [16], it was found that the slab-column connections presented a satisfactory strength to punching shear in order to withstand the loads that act on the intact structure. According to Table 2, the reactions and bending moments of the supports of the undamaged structure were obtained from the software SAP2000 [1].

**Table 2.** Reactions and the moments of the support in the structure without damage.

| Column | $N_k$ (kN) | $M_x$ (kNm) | $M_y$ (kNm) | Column | $N_k$ (kN) | $M_x$ (kNm) | $M_y$ (kNm) |
|---|---|---|---|---|---|---|---|
| P1 | 177.10 | 21.80 | 23.00 | P7 | 290.50 | 0.00 | 4.20 |
| P2 | 228.60 | 4.50 | 18.10 | P8 | 239.30 | 20.50 | 0.00 |
| P3 | 228.60 | 4.50 | 18.10 | P9 | 177.10 | 21.80 | 23.00 |
| P4 | 177.10 | 21.80 | 23.00 | P10 | 228.60 | 4.50 | 18.10 |
| P5 | 239.30 | 20.50 | 0.00 | P11 | 228.60 | 4.50 | 18.10 |
| P6 | 290.50 | 0.00 | 4.20 | P12 | 177.10 | 21.80 | 23.00 |

The effective depth (13 cm) and reinforcement ratio were determined according to the structural design presented at the reference. All connections presented studs type shear reinforcement, with four layers 6.23 cm$^2$ each at columns P1, P4, P9 and P12, and five layers 6.23cm$^2$ each for the other columns, spacing between studs equal to 10 cm and 6 cm from the first layer to the column face. Table 3 shows the shear stresses in the slab-column connections analyzed.

**Table 3.** Shear stresses at the critical section.

| Codes | Stress (MPa) | P1 | P2 | P6 |
|---|---|---|---|---|
| | $\tau_{rd3}$ | 0.70 | 0.74 | 0.78 |
| | $\tau_{sd3}$ | 0.48 | 0.48 | 0.57 |
| NBR 6118 | $\tau_{rd2}$ | 1.53 | 1.56 | 1.60 |
| | $\tau_{sd2}$ | 1.03 | 1.06 | 1.17 |
| | $\tau_{rd1}$ | 5.09 | 5.09 | 5.09 |
| | $\tau_{sd1}$ | 3.73 | 3.15 | 2.86 |
| | $\sigma_{rd3}$ | 0.58 | 0.61 | 0.64 |
| | $\sigma_{sd3}$ | 0.52 | 0.51 | 0.61 |
| EUROCODE | $\sigma_{rd2}$ | 1.42 | 1.45 | 1.48 |
| | $\sigma_{sd2}$ | 1.03 | 1.06 | 1.17 |
| | $\sigma_{rd1}$ | 5.28 | 5.28 | 5.28 |
| | $\sigma_{sd1}$ | 3.73 | 3.15 | 2.86 |
| | $v_{cout}$ | 0.70 | 0.70 | 0.70 |
| ACI | $V_{u2}$ | 0.43 | 0.43 | 0.52 |
| | $v_n$ | 2.17 | 2.17 | 2.17 |
| | $V_{u1}$ | 1.34 | 1.31 | 1.38 |

In Table 3:

- $\tau_{rd3}$ and $\tau_{sd3}$ are the strength and acting stresses outside the shear reinforcement,
- $\tau_{rd2}$ and $\tau_{sd2}$ are the strength and acting stresses at the shear reinforcement region,
- $\tau_{rd1}$ and $\tau_{sd1}$ are the strength and acting stresses at the periphery of the column,
- $\sigma_{rd3}$ and $\sigma_{sd3}$ are the strength and acting stresses outside the shear reinforcement,
- $\sigma_{rd2}$ and $\sigma_{sd2}$ are the strength and acting stresses at the shear reinforcement region,
- $\sigma_{rd1}$ and $\sigma_{sd1}$ are the strength and acting stresses at the periphery of the column,
- $v_n$ e $V_{u1}$ are the strength and acting stresses at the shear reinforcement region,
- $v_{cout}$ and $V_{u2}$ are the strength and acting stresses outside the shear reinforcement.

Figure 2 shows the acting and strength stresses ratio in the slab-column connections and as it can be seen, the analyzed supports present good punching shear strength, since the acting stresses were smaller than the capacity. EUROCODE [9] was the standard that presented the highest shear stress ratios in all the supports studied.

The possibility of progressive collapse is always relevant when the acting and the strength stresses ratio are high, not to mention the possibility of an overload or errors being done at the construction phase, for example. The highest ratios of the acting over the resistant stresses were taken as potential failures possibilities and the behavior of the floor slab and the remaining connections was then examined following these failures.

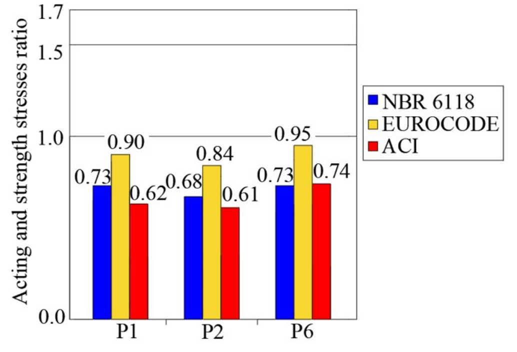


**Figure 2.** Acting and strength stresses ratio in the support.

### 3.1.2 Integrity reinforcement

Table 4 shows the integrity reinforcement designed according to the equations provided by the NBR 6118:2014 [10], GSA:2013 [17], CEB:2010 [8] and ACI 352:2011 [18] standards, basically considering the column reaction and the yield strength of the reinforcement.

Figure 3 shows a comparison between the amount of reinforcement found by the codes, with values being not so different, and ACI 352 [18] being surprisingly less conservative.

**Table 4.** Integrity reinforcement area.

| Column | $N_k$ *(kN)* | NBR 6118 (cm$^2$) | GSA (cm$^2$) | CEB (cm$^2$) | ACI (cm$^2$) |
|---|---|---|---|---|---|
| P1 | 177.10 | 7.33 | 10.81 | 8.23 | 6.46 |
| P2 | 228.60 | 9.46 | 10.81 | 10.62 | 6.46 |
| P6 | 290.50 | 12.03 | 10.81 | 13.50 | 6.46 |

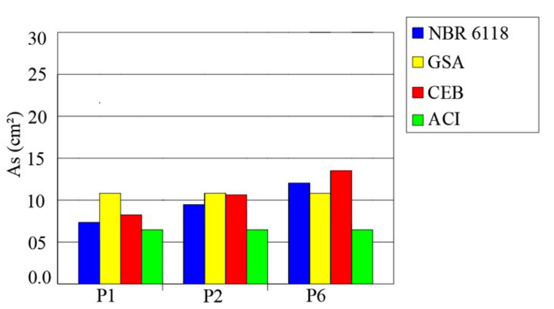


**Figure 3.** Comparison of reinforcement steel area.

### 3.1.3 Post punching shear pattern

After a punching shear failure at an internal slab-column connection, the possibility of a new punching failure at the neighboring connections was verified, considering zero or a partial residual strength at the damaged support. Table 5 shows the columns reactions when a punching failure is admitted at edge column P2.

**Table 5.** Reactions and bending moments of support after P2 punching shear.

| Column | $N_k$ (kN) | $M_x$ (kNm) | $M_y$ (kNm) | Column | $N_k$ (kN) | $M_x$ (kNm) | $M_y$ (kNm) |
|---|---|---|---|---|---|---|---|
| P1 | 271.00 | 127.10 | 17.30 | P7 | 267.80 | 7.30 | 1.90 |
| P2 | - | - | - | P8 | 235.70 | 19.00 | 0.90 |
| P3 | 349.40 | 74.80 | 18.90 | P9 | 172.10 | 11.30 | 20.90 |
| P4 | 158.20 | 20.50 | 13.90 | P10 | 207.90 | 4.30 | 5.70 |
| P5 | 208.20 | 30.90 | 13.20 | P11 | 223.40 | 4.50 | 12.20 |
| P6 | 411.20 | 10.90 | 42.40 | P12 | 178.90 | 22.60 | 23.70 |

Figure 4 shows the columns reactions changes for the neighbor's connections following a punching shear failure at column P2, compared with the intact structure. Only the most affected columns connections are shown, together with column P12, far from column P2, for comparison.

As seen, with a total failure at P2 column connection a load increase of 53.0% is obtained at column P1, or an increase of 45.1% is obtained with a residual strength of 15% at column P2, stating the high probability of the occurrence of new failures in sequence, not to mention that the bending moments increased more than five times at P1 connection.

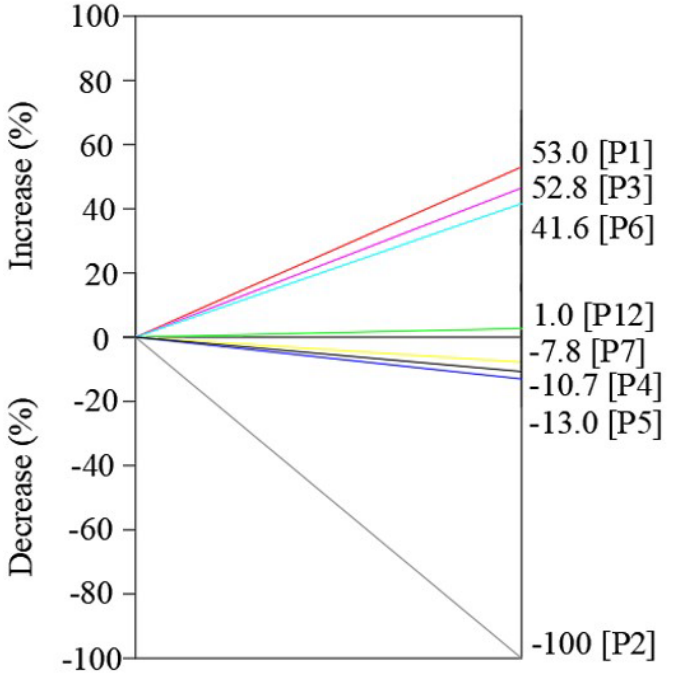


**Figure 4.** Variation of support reactions after failure at P2.

Integrity reinforcement at the failed slab-column connection can provide up to 60% residual strength, according to experimental research carried out by Melo [6], and by Lima [22] at the University of Brasília, allowing that failed connection can withstand more load and less load being spread to the other supports.

Big increases are always found at the "first neighbor line" supports close to a failed connection, as was seen at column connections P1 and P3 after failure at column connection P2. At a "second neighbor line" the load decrease, as seen at column connections P5 and P7. On the other hand, column connection P12, that is far from the failure has only a small increase in its load, as seen in Figure 4.

Table 6 shows the shear stresses for the internal slab-column connection P1, considering a zero or partial residual strength at the damaged connection, after a punching shear failure at connection P2.

The possibility of progressive collapse in the building would be avoided if the acting and strength stress ratio would be less than one, the defined limit, guaranteeing that the remaining strength is bigger than the actual acting load.

**Table 6.** Shear stresses in P1 after failure at P2.

| Codes | Stress (MPa) | P1 No residual reaction in P2 | P1 60% of residual reaction in P2 |
|---|---|---|---|
| | $\tau_{rd3}$ | 0.70 | 0.70 |
| | $\tau_{sd3}$ | 0.93 | 0.66 |
| NBR 6118 | $\tau_{rd2}$ | 1.53 | 1.53 |
| | $\tau_{sd2}$ | 2.19 | 1.50 |
| | $\tau_{rd1}$ | 5.09 | 5.09 |
| | $\tau_{sd1}$ | 9.34 | 6.02 |
| | $\sigma_{rd3}$ | 0.58 | 0.58 |
| | $\sigma_{sd3}$ | 0.98 | 0.70 |
| EUROCODE | $\sigma_{rd2}$ | 1.42 | 1.42 |
| | $\sigma_{sd2}$ | 2.19 | 1.50 |
| | $\sigma_{rd1}$ | 5.28 | 5.28 |
| | $\sigma_{sd1}$ | 9.34 | 6.02 |
| | $v_{cout}$ | 0.70 | 0.70 |
| ACI | $V_{u2}$ | 0.79 | 0.58 |
| | $v_n$ | 2.17 | 2.17 |
| | $V_{u1}$ | 2.97 | 2.00 |

Figure 5 shows the acting and strength stresses ratios at the column P1, considering a residual strength of 0% or 60% at P2, aiming to verify the post-punching shear behavior of the analyzed structure.

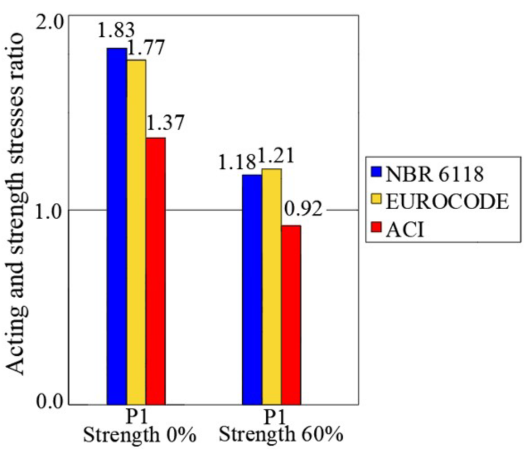


**Figure 5.** Shear stresses ratio in P1 for zero and for 60% of residual reaction in P2.

It is seen that according to NBR6118 [10] and EUROCODE [9] standards there is a great possibility of new punching shear failures in the structure, even with the presence of integrity reinforcement at P2, due to the large increase in reaction at P1.

### 3.1.4 Estimating the floor remaining capacity following a punching shear failure by the Yield Line Theory

The flexural capacity of the slab was determined after punching shear failure of a slab-column connection close to the edge (P2), without considering any residual strength. After the loss of support in the structure, the loads were redistributed to the columns, with an increase or decrease in reactions.

The Yield Line Method is applied for calculating the remaining capacity of the floor after a shear punching had occurred, taking in account all the well anchored flexural reinforcement according to the structural concrete requirements that crosses the supposed yield line rupture mechanisms and then can provide yielding resisting moment.

As seen in Figure 6, one possible yield line pattern is adopted after a punching shear had occurred in P2 connection, the Virtual Work Principle is used to calculate the remaining capacity of the floor by the Yield Line Method, assuming a virtual unitary displacement at the point “J”, in this case where the slab/column connection failed, and all the contributions of the hogging and sagging reinforcement is considered, provide it is well anchored and crosses the yield lines. The volume of the deformed shape when the virtual unitary displacement (J) is applied is shown in Figure 7, considering the rotations of the floor.

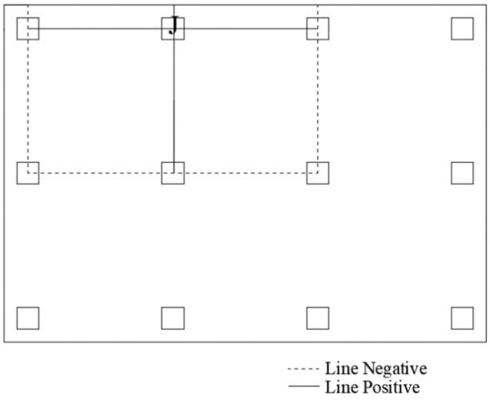


**Figure 6.** Positive and negative yield line configuration.

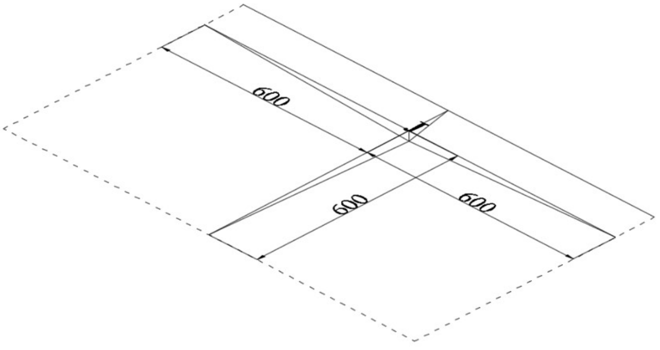


**Figure 7.** Deformation of a slab – Dimensions in cm.

Figures 8, 9, 10 and 11 show the positive and negative yielding resisting moments strengths of the floor slab, determined taking in account all the well anchored flexural reinforcement that crosses the assumed yield line pattern.

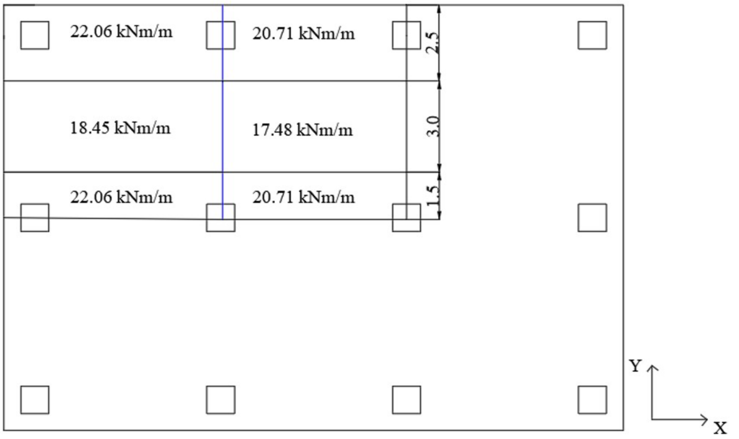


**Figure 8.** Positive moment strengths in the X direction – Dimensions in m.

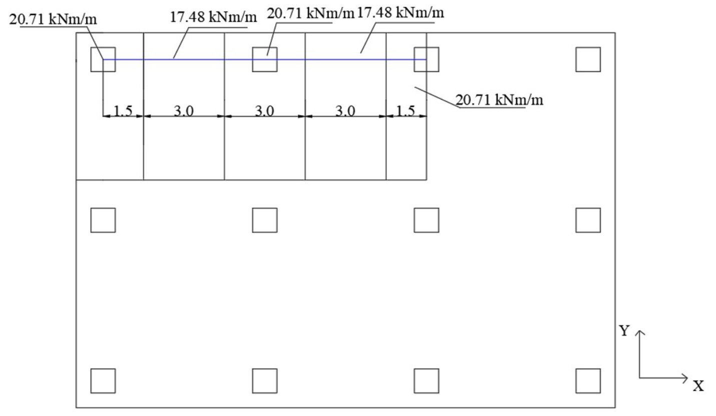


**Figure 9.** Positive moment strengths in the Y direction – Dimensions in m.

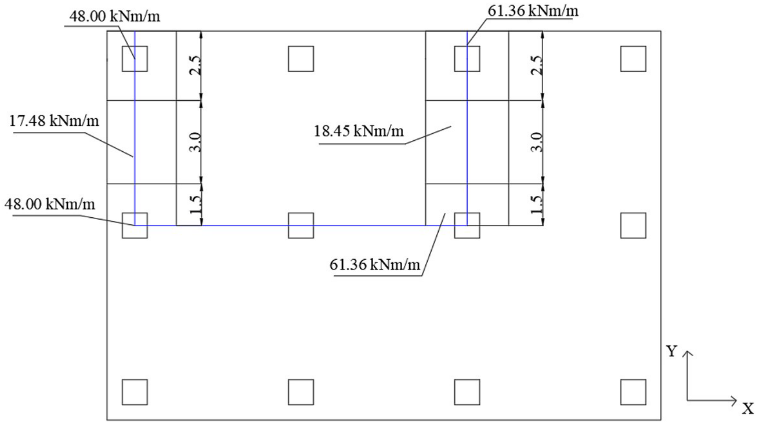


**Figure 10.** Negative moment strengths in the X direction – Dimensions in m.

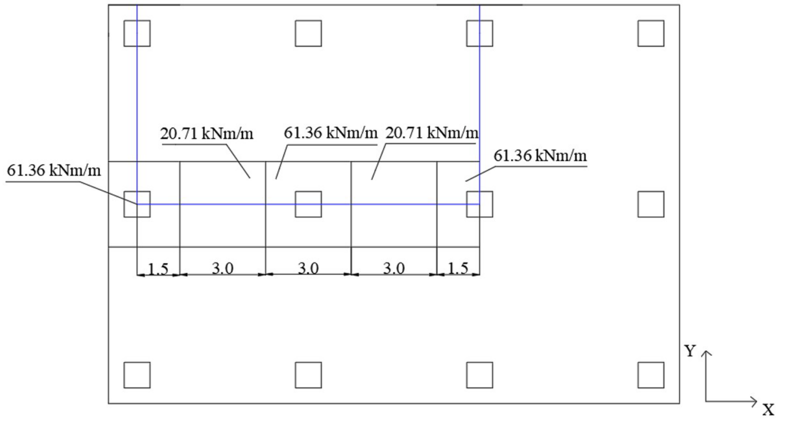


**Figure 11.** Negative moment strengths in the Y direction – Dimensions in m.

As seen the Yield Line Method can be calculated by the Virtual-Work Method considering the external work required by the load and the internal work used by the slab or floor to deform itself.

The external work required by a load applied uniformly on a slab can be determined by the product of the failure load and the volume of the displaced slab after the application of the virtual displacement. The internal work can be defined as the product of the strength moments and rotations in the slab [23].

The calculated collapse load (5.39 kN/m$^2$) was 44% lower than the predicted actual load on the slab (9.58 kN/m$^2$), after the loss of support P2, stating the real and big possibility of the occurrence of progressive collapse in the structure.

As Yield Line is a Superior Limit Method [23]–[25] other possible collapse mechanism could have been found with an even lower collapse load but there is no need for this search as the floor slab is already in a critical condition for the possibility of occurrence of a progressive collapse for the one yield line pattern investigated.

As was seen the Yield Line Method can be applied to verify the possibility of a progressive collapse following a punching shear failure at a connection. It should also be mentioned that for this analysis no residual strength at the damaged slab-column connection was considered. If integrity reinforcement at P2 was considered the situation would be less severe, as the collapse load would be higher.

### 3.2 Second Example

The studied building was designed in 2015 [26] and its post-punching shear behavior was analyzed using the software for structural design in reinforced concrete Eberick [2], using “Grid Analogy”, basically with plate elements connected to bars in two orthogonal directions presenting bending stiffness that can be adjusted.

The building structure has six floors, with a garage parking on the third floor formed by a 35 cm thick waffle slab and a ceiling height of 270 cm, two rigid cores formed by the stairs and elevator shaft, and floor openings for hydro-sanitary pipes. There is also a car access ramp at the left corner and presence beams connecting the columns at the periphery of the building.

The slab / column connections located at the third floor of the building were studied. Concrete with 30 MPa strength were adopted, and a cross-section of the ribbed slab and the floor plan of the structure are shown respectively in Figures 12 and 13.

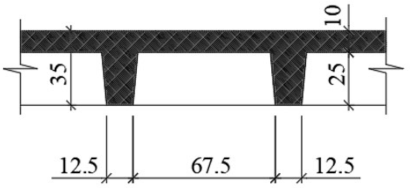


**Figure 12.** Section of the waffle slab – Dimensions in cm.

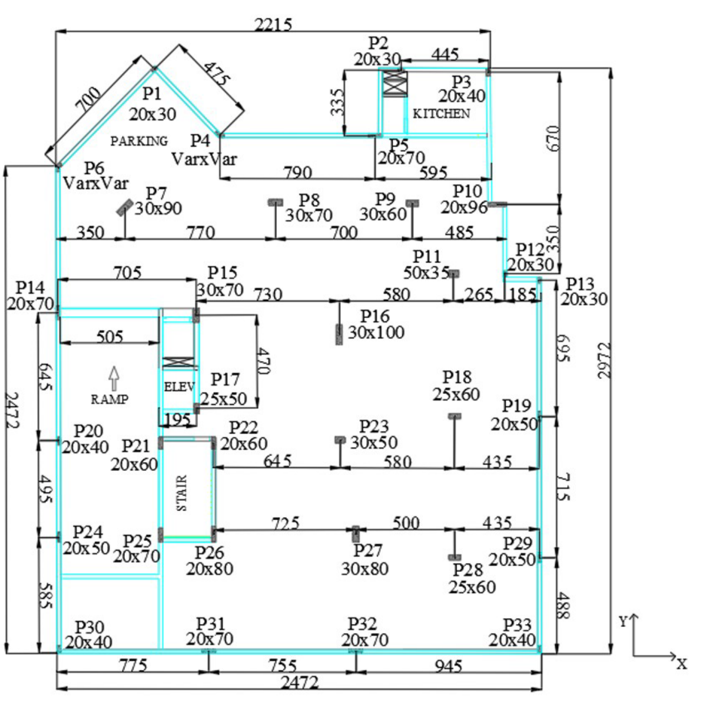

**Figure 13.** Floor plan of the parking – Dimensions in cm.

Horizontal forces from wind action were considered on the structure according to NBR 6123 [27], and Table 7 presents the gravity loads adopted at the structural design, according to NBR 6120 [21]. A live load of 5.0 kN/m$^2$ and a dead load of 6.02 kN/m$^2$ were used on the floor slab of the third floor.

**Table 7.** Load used.

| Overview | Amount |
|---|---|
| Dead Load (distributed): | Load (kN/m$^2$) |
| Self-weight of slab | 4.60 |
| Cladding | 1.23 |
| Wall | 0.19 |
| Live Load: | Load (kN/m$^2$) |
| Load in parking building | 5.00 |

### 3.2.1 Punching shear assessment

Punching shear was checked at three internal slab columns connections (P11, P23 and P27) of the intact structure, susceptible to punching shear failures, and according to the shear stresses obtained by the codes NBR 6118:2014 [10], EUROCODE 2:2004 [9] and ACI 318:2019 [16].

Table 8 shows all columns reactions and bending moments for the intact structure, calculated by the Eberick software [2]. Columns P11, P23 and P27 have respectively cross sections of 50 cm x 35 cm, 50 cm x 30 cm and 80 cm x 30 cm.

**Table 8.** Reactions and the moments of the support in the structure without damage.

| Column | $N_k$ (kN) | $M_x$ (kNm) | $M_y$ (kNm) | Column | $N_k$ (kN) | $M_x$ (kNm) | $M_y$ (kNm) |
|---|---|---|---|---|---|---|---|
| P1 | 117.30 | 9.50 | 28.30 | P18 | 465.70 | 3.50 | 30.10 |
| P2 | 99.60 | 18.10 | 4.00 | P19 | 220.40 | 0.30 | 14.10 |
| P3 | 134.90 | 15.50 | 44.40 | P20 | 82.90 | 5.40 | 41.30 |
| P4 | 156.80 | 31.50 | 18.80 | P21 | 128.10 | 7.50 | 35.90 |
| P5 | 215.00 | 34.30 | 9.50 | P22 | 193.00 | 10.20 | 39.10 |
| P6 | 145.90 | 11.40 | 26.90 | P23 | 415.70 | 1.30 | 57.30 |
| P7 | 546.40 | 83.60 | 23.50 | P24 | 163.40 | 11.30 | 65.20 |
| P8 | 500.70 | 33.50 | 20.50 | P25 | 240.30 | 13.60 | 102.60 |
| P9 | 332.90 | 6.00 | 43.30 | P26 | 317.90 | 9.00 | 29.20 |
| P10 | 159.70 | 39.60 | 40.90 | P27 | 530.00 | 25.70 | 107.30 |
| P11 | 332.10 | 20.20 | 15.70 | P28 | 424.30 | 3.40 | 33.90 |
| P12 | 56.90 | 1.90 | 6.20 | P29 | 186.40 | 4.40 | 36.20 |
| P13 | 86.30 | 4.60 | 28.30 | P30 | 153.60 | 27.80 | 40.90 |
| P14 | 243.40 | 31.90 | 54.20 | P31 | 278.30 | 59.40 | 0.60 |
| P15 | 373.90 | 75.50 | 31.80 | P32 | 255.40 | 48.40 | 1.40 |
| P16 | 590.70 | 20.50 | 69.10 | P33 | 131.00 | 35.30 | 19.70 |
| P17 | 173.10 | 9.10 | 45.60 | - | - | - | - |

The top flexural reinforcement was 12.5 mm bars each ten centimeters and 16 mm bars each fifteen centimeters respectively for the x and y directions for column P11 connection, 12.5 mm bars each ten centimeters for the two directions for column P23 connection, and 16 mm bars each ten centimeters and 12.5 mm bars each ten centimeters respectively for the x and y directions for column P27 connection.

For the bottom flexural reinforcement was 10 mm bars each ten centimeters for the two directions for column P11 and P27 connections, and 10 mm bars each fifteen centimeters for the two directions for column P23 connection. For the ribs 12.5- or 16-mm bars were used at the bottom and 12.5 mm at the top at the two directions.

Shear reinforcement was present at all internal connections, designed by the NBR 6118 [10], in four layers, each with 4.36 cm$^2$ for the regions of columns P11 and P23, and with 4.98 cm$^2$ for the region of column P27, the first layer being 16 cm from the column and the others 24 cm apart.

Table 9 presents the acting and strength stress at the studied connections, according to the three codes presented, and Figure 14 presents the stress ratio for verifying the stability of the structure. It can be seen that the strength capacity is higher than the actual acting load for all three the studied columns regions, and the structure can be considered safe.

Connections at columns P11, P23 and P27 were chosen as are susceptible to punching shear failures even though P27 would be the most susceptible as seen in Figure 14.

**Table 9.** Shear stresses at the critical section.

| Codes | Stress (MPa) | P11 | P23 | P27 |
|---|---|---|---|---|
| | $\tau_{rd3}$ | 0.52 | 0.51 | 0.56 |
| | $\tau_{sd3}$ | 0.15 | 0.19 | 0.24 |
| NBR 6118 | $\tau_{rd2}$ | 0.61 | 0.61 | 0.65 |
| | $\tau_{sd2}$ | 0.31 | 0.40 | 0.52 |
| | $\tau_{rd1}$ | 5.09 | 5.09 | 5.09 |
| | $\tau_{sd1}$ | 1.29 | 2.00 | 1.99 |
| | $\sigma_{rd3}$ | 0.48 | 0.48 | 0.52 |
| | $\sigma_{sd3}$ | 0.16 | 0.20 | 0.26 |
| EUROCODE | $\sigma_{rd2}$ | 0.52 | 0.52 | 0.55 |
| | $\sigma_{sd2}$ | 0.31 | 0.40 | 0.52 |
| | $\sigma_{rd1}$ | 5.28 | 5.28 | 5.28 |
| | $\sigma_{sd1}$ | 1.29 | 2.00 | 1.99 |
| | $v_{cout}$ | 0.66 | 0.66 | 0.66 |
| ACI | $V_{u2}$ | 0.14 | 0.17 | 0.22 |
| | $v_n$ | 1.17 | 1.18 | 1.17 |
| | $V_{u1}$ | 0.43 | 0.58 | 0.69 |

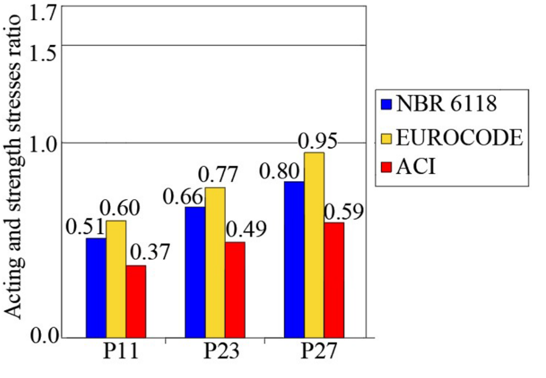


**Figure 14.** Acting and strength stresses ratio in support.

Estimations with NBR 6118 [10] and EUROCODE [9] are close, as the acting shear stresses are calculated in almost the same way, while the resisting shear stresses differs as the European code has a higher safety factor for the concrete strength and limits the top reinforcement ratio and the size effect.

### 3.2.2 Integrity reinforcement

The Table 10 shows the results obtained by the NBR 6118:2014 [10], GSA:2013 [17], CEB:2010 [8] and ACI 352:2011 [18] codes, for the integrity reinforcement steel areas. The most conservative standard was found, while Figure 15 shows a comparison of the reinforcement areas.

**Table 10.** Integrity reinforcement area.

| Column | $N_k$ *(kN)* | NBR 6118 (cm$^2$) | GSA (cm$^2$) | CEB (cm$^2$) | ACI (cm$^2$) |
|---|---|---|---|---|---|
| P11 | 332.10 | 13.75 | 25.55 | 15.43 | 5.62 |
| P23 | 415.70 | 17.21 | 25.55 | 19.32 | 4.67 |
| P27 | 530.00 | 21.94 | 25.55 | 24.63 | 5.77 |

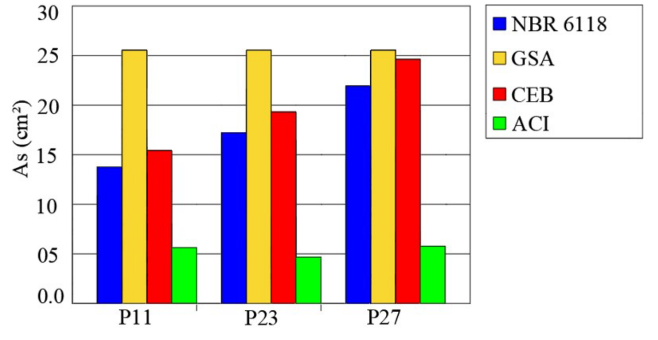


**Figure 15.** Comparison of reinforcement steel areas.

It can be seen that the GSA [17] standard is the most conservative in all cases, presenting the largest reinforcement areas against progressive collapse, leading to a possibly lower possibility of propagation of a collapse. For P11 it is observed that the GSA standard [17] has a steel area 86% larger than the Brazilian standard NBR 6118 [10], as the GSA [17] does not consider the support reactions in the calculation of the reinforcement, while for P27 the difference is small difference between GSA [17] and CEB [8].

### 3.2.3 Post punching shear pattern

The analysis of the post punching shear behavior of the slab studied was carried out considering as previous a total or partial loss of a slab-column connection after a punching shear failure, comparing the bending moments and column reactions, and checking the possibility of the damage being spread through other connections.

Table 11 shows changes in reaction and in bending moments when slab-column connection P23 is removed, and Figure 16 shows the internal connections with the highest variations in percentage.

**Table 11.** Reactions and moments of support after P23 punching shear.

| Column | $N_k$ *(kN)* | $M_x$ *(kNm)* | $M_y$ *(kNm)* | Column | $N_k$ *(kN)* | $M_x$ *(kNm)* | $M_y$ *(kNm)* |
|---|---|---|---|---|---|---|---|
| P1 | 116.70 | 9.30 | 27.90 | P17 | 182.30 | 7.20 | 50.10 |
| P2 | 99.60 | 18.10 | 3.30 | P18 | 520.00 | 3.20 | 27.60 |
| P3 | 134.60 | 15.50 | 43.6 | P19 | 210.10 | 0.20 | 18.20 |
| P4 | 158.50 | 32.20 | 19.4 | P20 | 82.40 | 5.70 | 46.60 |
| P5 | 217.40 | 33.80 | 10.50 | P21 | 117.10 | 7.90 | 38.10 |
| P6 | 145.40 | 10.80 | 27.3 | P22 | 220.10 | 8.50 | 35.10 |
| P7 | 545.00 | 82.90 | 23.3 | P23 | - | - | - |
| P8 | 486.40 | 30.00 | 22.60 | P24 | 164.50 | 12.10 | 63.50 |
| P9 | 325.00 | 7.60 | 40.40 | P25 | 242.60 | 16.00 | 99.70 |
| P10 | 160.50 | 39.30 | 43.40 | P26 | 334.60 | 10.40 | 36.80 |
| P11 | 325.70 | 20.30 | 12.10 | P27 | 714.30 | 34.70 | 105.40 |
| P12 | 58.40 | 1.90 | 5.90 | P28 | 415.00 | 1.90 | 41.00 |
| P13 | 85.20 | 4.70 | 26.70 | P29 | 185.00 | 4.20 | 38.30 |
| P14 | 242.30 | 32.00 | 59.80 | P30 | 155.40 | 28.10 | 43.00 |
| P15 | 379.40 | 74.60 | 30.60 | P31 | 273.40 | 54.20 | 0.50 |
| P16 | 752.10 | 25.20 | 158.6 | P32 | 245.60 | 55.70 | 1.20 |
| - | - | - | - | P33 | 130.90 | 34.50 | 22.20 |

Column P23 was chosen to be removed to guarantee high loads at neighboring internal slab-column connections, more susceptible to punching shear failures, and avoiding the periphery columns with beams.

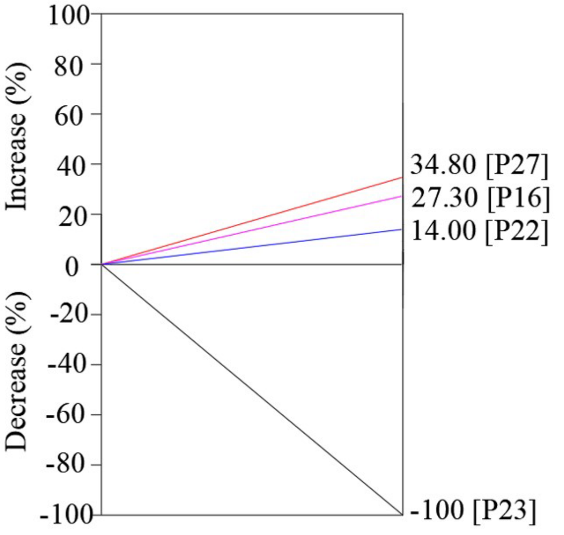


**Figure 16.** Variation of support reactions after failure at P23.

As seen in figure 16 the most loaded support following a failure at P23 is slab / column connection P27, presenting a 34.8% load increase in comparison with the intact structure, and is investigated.

Considering a residual strength of 15% in connection P23 the load increase in P27 drops to 29.6%, possibly still a high value that could contribute to spread the failure. With integrity reinforcement the residual strength could go up to 60%, reducing the load increase to 13.9% at P27, practically putting aside the possibility of progressive collapse with a 15% residual strength at connection P23 and the presence of the integrity reinforcement.

Table 12 shows the punching shear stresses in the region of slab column connection P27 when zero or 60% residual strength is considered for connection P23, and Figure 17 shows the comparison between the actual acting load and the strength capacity for these simulations.

It can be seen that the integrity reinforcement is effective in reducing the acting and strength stress ratio, preventing the possibility of a progressive collapse in the building, according to the NBR 6118 [10] and ACI 318 [16] standards.

**Table 12.** Shear stresses in P27 after failure at P23.

| Codes | Stress (MPa) | P27 No residual reaction in P23 | P27 60% of residual reaction in P23 |
|---|---|---|---|
| | $\tau_{rd3}$ | 0.56 | 0.56 |
| | $\tau_{sd3}$ | 0.32 | 0.27 |
| NBR 6118 | $\tau_{rd2}$ | 0.65 | 0.65 |
| | $\tau_{sd2}$ | 0.67 | 0.58 |
| | $\tau_{rd1}$ | 5.09 | 5.09 |
| | $\tau_{sd1}$ | 2.45 | 2.18 |
| | $\sigma_{rd3}$ | 0.52 | 0.52 |
| | $\sigma_{sd3}$ | 0.34 | 0.29 |
| EUROCODE | $\sigma_{rd2}$ | 0.55 | 0.55 |
| | $\sigma_{sd2}$ | 0.66 | 0.58 |
| | $\sigma_{rd1}$ | 5.28 | 5.28 |
| | $\sigma_{sd1}$ | 2.45 | 2.18 |
| | $v_{cout}$ | 0.66 | 0.66 |
| ACI | $V_{u2}$ | 0.29 | 0.25 |
| | $v_n$ | 1.17 | 1.17 |
| | $V_{u1}$ | 0.88 | 0.77 |

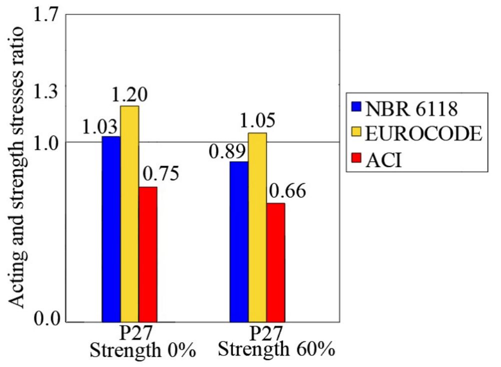


**Figure 17.** Shear stresses ratio in P27 for zero and for 60% of residual reaction in P23.

### 3.2.4 Predicting the floor remaining capacity following a punching shear failure by the Yield Line Theory

Assuming that there was a punching shear failure at P23, the flexural capacity of the slab was calculated and the possibility of a progressive collapse in the structure was checked, as the Yield Line Method is applied for calculating the remaining capacity of the floor after a punching shear had occurred, taking in account all the well anchored flexural reinforcement, according to the structural concrete requirements, that crosses the supposed yield line rupture mechanisms and then can provide yielding resisting moment. Yield lines were drawn considering that the collapse would be restricted around the damaged slab column region. Figure 18 presents a yield line pattern considering a possible slab collapse scenario, assuming negative lines connecting P16, P18, P27 and P22, and a positive line connecting P16, P23 and P27.

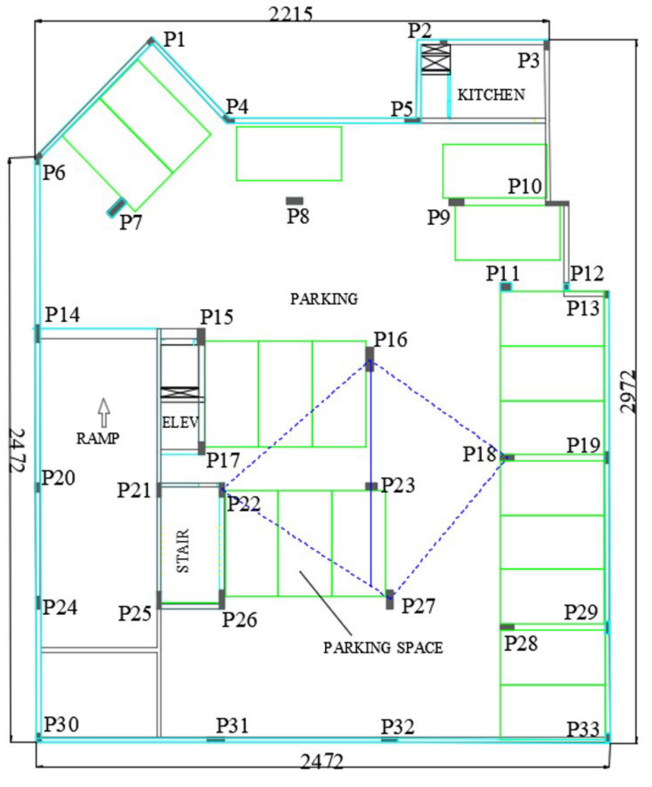


**Figure 18.** Positive and negative yield line configuration.

As seen in Figure 19, after a possible yield line pattern is adopted after a shear punching had occurred, the Virtual Work Principle is used to calculate the remaining capacity of the floor by the Yield Line Method, assuming a virtual unitary displacement at the point "J", in this case where the slab/column connection failed, and all the contributions of the hogging and sagging reinforcement is considered, provide it is well anchored and crosses the yield lines. The volume of the deformed shape when the virtual unitary displacement (J) is applied is shown in the figure, considering the rotations or deformations of the floor.

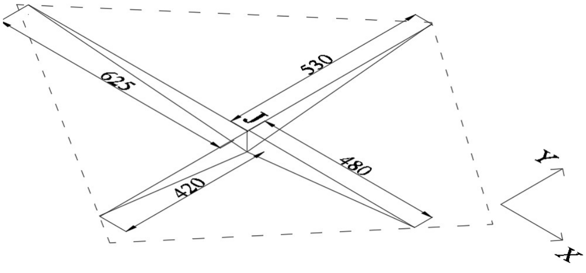


**Figure 19.** Deformations of slab – Dimensions in cm.

Figures 20, 21 and 22 show the positive and negative yielding resisting moments strengths of the floor slab, determined taking in account all the well anchored flexural reinforcement that crosses the assumed yield line pattern.

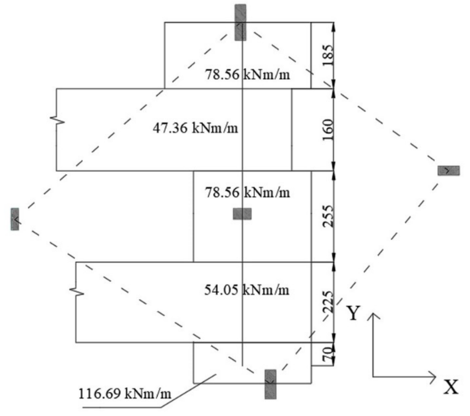


**Figure 20.** Positive moment strengths in the X direction – Dimensions in cm.

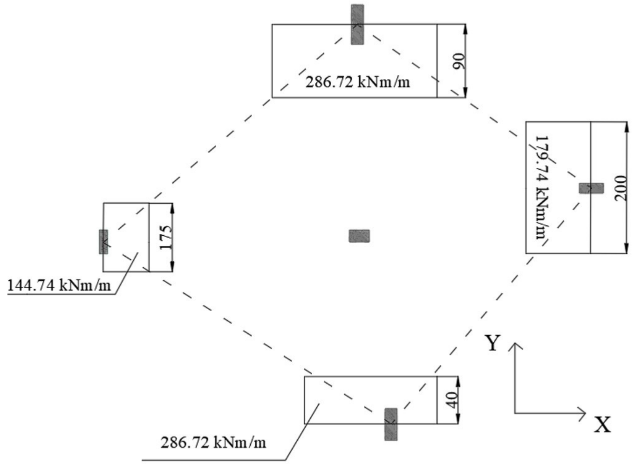


**Figure 21.** Negative moment strengths in the X direction – Dimensions in cm.

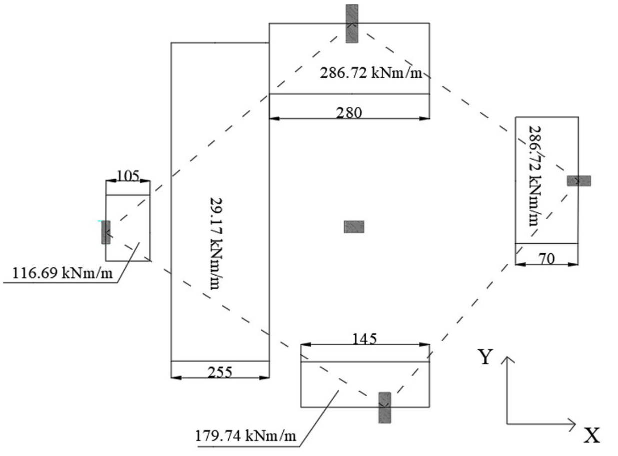


**Figure 22.** Negative moment strengths in the Y direction – Dimensions in cm.

As in the previous example the Virtual-Work Method was used to calculate the flexural remaining capacity of the floor and was estimated as 25.10 kN/m$^2$, more than double of the actual acting load on the flat slab (11.02 kN/m$^2$), with practically no possibility of progressive collapse for this yield line pattern tested.

Having said that, as the Yield Line is a Superior Limit Method another yield line patterns should be tested before the possibility of a progressive collapse could have been disregarded.

As seen the Yield Line Method can be applied to verify the possibility of a progressive collapse following a punching shear failure at a connection.

## 4 CONCLUSIONS

The possibility of a second punching failure in sequence and of a progressive collapse following a column connection punching shear failure was investigated on a flat slab floor building with 20 x 14 meters in plan with three stories and twelve columns (Example 1) and on a waffle slab floor building with 25 x 30 meters in plan with six stories and thirty-three columns (Example 2).

Following a punching shear failure at the most loaded column connection, the remaining most loaded connection was checked for a punching shear failure, considering that the first failed column connection could hold zero or 60% of its original load, assuming that the connection could hold this amount of its original load when well designed and detailed integrity bottom reinforcement was installed at the column connection. The possibility of a progressive collapse at the slab floors after punching shear failures had occurred was then checked using the Yield Line Method [6], [7], [11], [22].

Regarding the possibility of a second punching shear failure in sequence, when there is no Integrity Reinforcement at the failed connection and it cannot hold any load, the three codes (ACI 318 [16], EUROCODE [9] and NBR 6118 [10]) indicate the possibility of a second punching shear failure in sequence for the first example, while only EUROCODE [9] and NBR 6118 [10] indicate this possibility for the second example. However, when Integrity Reinforcement well designed and detailed was present at the column connection only codes EUROCODE [9] and NBR 6118 [10] indicate the possibility a second punching shear failure in sequence for the first example, while only EUROCODE [9] indicates this possibility for the second example.

In respect to the occurrence of a Progressive Collapse of the floor slabs following the punching shear failure, investigated by the Yield Line Method and depending on the remaining capacity and the flexural resistance of the floors, it was shown that progressive collapse would have happen only for the first example, as the load applied would be about two times higher than the resistance of the floor. For the second example the resistance of the floor slab was more than double the applied load, securing it against the possibility of a progressive collapse.

As a general conclusion can be stated that slab column connections should be designed and detailed to prevent Progressive Collapse even when a punching shear failure had occurred in one of the connections. The post punching shear resistance of the top (hogging) bending reinforcement is low, but well anchored bottom bars going through the column (Integrity Reinforcement) can improve up to 60% the residual capacity of the connection [6], [7], [11], [22].

And that in flat slabs or plates the global behavior, the possibility of progressive collapse following a punching shear failure, and the remaining capacity of the floors depends on the *i)* post-punching resistance of the connection being punched; *ii)* post-punching resistance of the neighbors' connections; *iii)* flexural resistance of the slabs, and that it can be well estimated by the Yield Line Method.

## ACKNOWLEDGEMENTS

The authors would like to thank the University of Brasilia, CAPES - Coordenação de Aperfeiçoamento de Pessoal de Nível Superior, CNPq - Conselho Nacional de Desenvolvimento Científico e Tecnológico, and FAP-DF - Fundação de Apoio à Pesquisa do Distrito Federal, Brazilian Research Development Agencies, for the support of this research.

## REFERENCES

[1] Computers and Structures, Inc., *Static and Dynamic Finite Element Analysis of Structure*, SAP2000 16, 2014.

[2] Eberick, *Reinforced Concrete Structural Design Software. AltoQi*, 2022.

[3] P. A. Martins, "Colapso progressivo em edifícios em laje cogumelo de concreto armado," M.S. thesis, UnB, Brasíla, DF, 2003.

[4] H. I. Longo, "Análise da estrutura para avaliação do colapso progressivo," in *VII CBPE Conference*, 2014, pp. 1-10.

[5] H. Jaroslav, V. Aleksandar, and B. Viktor, "Failure analysis of collapsed parking garage building due to punching," *Eng. Fail. Anal.*, vol. 129, pp. 105712, Sep 2021, http://dx.doi.org/10.1016/j.engfailanal.2021.105712.

[6] G. S. S. A. Melo, "Behavior of reinforced concrete flat slabs after local failure," Ph.D. dissertation, Polytech. Centr. London, London, 1990.

[7] G. S. Melo and P. E. Regan, "Post-punching resistance of connections between flat slabs and interior columns," *Mag. Concr. Res.*, vol. 50, no. 4, pp. 319–327, Dec 1998, http://dx.doi.org/10.1680/macr.1998.50.4.319.

[8] International Federation for Structural Concrete, *Model Code for Concrete Structures*, 2010.

[9] European Committee for Standardization, *Design of Concrete Structures: General Rules and Rules for Buildings*, EUROCODE 2, 2004.

[10] Associação Brasileira de Normas Técnicas, *Projeto de estruturas de concreto*, NBR 6118, 2014.

[11] G. S. Melo and P. E. Regan, "Post-punching behavior of a waffle flat slab floor," in *Proc. 1st Int. Conf. Fract. Mech. Concr. Struct.*, 1992, https://doi.org/10.1201/9781482286847.

[12] K. V. Udilovich, I. B. Shleykov, and M. V. Banchuzhnyy, "Design of flat-plate floors for progressive collapse using yield-line analysis," *Concr. Int.*, vol. 32, no. 7, pp. 1–8, Jul 2010. Accessed: Jun. 23, 2022. [Online]. Available: https://www.concrete.org/publications/internationalconcreteabstractsportal/m/details/id/51663822

[13] M. Byfield, W. Mudalige, C. Morison, and E. Stoddart, "A review of progressive collapse research and regulations," *Proc. Inst. Civ. Eng., Struct. Build.*, vol. 167, no. 8, pp. 447–456, 2014, http://dx.doi.org/10.1680/stbu.12.00023.

[14] J. Garzón-roca, J. Sagaseta, M. Buitrago, and J. M. Adam, "Dynamic punching assessment of edge columns after sudden corner column removal," *ACI Struct. J.*, vol. 118, no. 2, pp. 299–311, Mar 2021, http://dx.doi.org/10.14359/51728195.

[15] S. A. E. Kakhki, A. Kheyroddin, and A. Mortezaei, "Evaluation of the progressive collapse of the reinforced concrete frames considering the soil–structure interaction: parametric study based on the sensitivity index," *Int. J. Concr. Struct. Mater.*, vol. 16, no. 38, pp. 1–24, 2022, http://dx.doi.org/10.1186/s40069-022-00523-x.

[16] American Concrete Institute, *Building Code Requirements for Structural Concrete and Commentary*, ACI 318, 2019.

[17] U.S. General Services Administration, *Alternate Path Analysis & Design Guidelines for Progressive Collapse Resistance*, 2013.

[18] American Concrete Institute, *Guide for Design of Slab-Column Connections in Monolithic Concrete Structures Standards*, ACI 352, 2011.

[19] R. A. Chaves, *Concreto Armado II – Lajes lisas e Lajes cogumelo*. Belo Horizonte: UFMG, 2011.

[20] N. A. Silva, *Concreto Armado II – Especialização*. Belo Horizonte: UFMG, 2015.

[21] Associação Brasileira de Normas Técnicas, *Cargas para o cálculo de estruturas de edificações*, NBR 6120, 1980.

[22] A. F. Lima No., "Análise experimental na fase de pós-puncionamento de lajes cogumelo de concret," M.S. thesis, UnB, Brasíla, DF, 2003

[23] K. W. Johansen, *Linhas de Ruptura: teoria e prática*, 1ª ed. Curitiba: Editora LT, 1962.

[24] J. D. Lima, A. T. Coelho, and V. Monteiro, *Manual de Betão Armado*, 5ª ed. Lisboa: Editora LNEC, 1980.

[25] B. Balakrishnan and D. Menon, "Collapse load estimation of rectangular RC beam-slab systems: new insights," *ACI Struct. J.*, vol. 115, no. 5, pp. 1279–1294, 2018, http://dx.doi.org/10.14359/51702246.

[26] E. M. Piancastelli, *Design of Reinforced Concrete Structure in DWG AutoCAD Software*, 2021.

[27] Associação Brasileira de Normas Técnicas, *Forças Devidas ao Vento em Edificações*, ABNT NBR 6123, 1988.

**Author contributions:** The second author of this article was the supervisor of the research accomplished by the first author during his MSc Thesis.

**Editors:** Diogo Rodrigo Ribeiro, Guilherme Aris Parsekian.